AIMS Biophysics

AIMS Biophysics, 7(2): 90–118.
DOI: 10.3934/biophy.2020008
Received: 26 February 2020
Accepted: 16 April 2020
Published: 23 April 2020

http://www.aimspress.com/journal/biophysics

Review

Strategies to investigate protein turnover with fluorescent protein reporters in eukaryotic organisms

Jonathan Trauth, Johannes Scheffer, Sophia Hasenjäger and Christof Taxis*

Molecular Genetics, Department of Biology, Philipps-University Marburg, Germany

*** Correspondence:** Email: taxis@staff.uni-marburg.de; Tel: +4964212823046.

Abstract: In higher eukaryotes, defects in regulated protein turnover are intimately linked to development of diseases and aging. Systematic investigation of proteostasis and protein degradation pathways is of high importance for understanding basic cellular events as well as developmental processes in higher organisms. Recently, novel fluorescent protein-based tools for monitoring protein degradation and mapping degradation pathways were described that facilitate this task. Here we give an overview of these tools and relate them to biophysical properties of fluorescent proteins. We focus on methods for the identification of degradation pathways, the discovery of novel degradation sequences, the investigation of proteome dynamics, and the characterization of protein stability. One can expect systematic application of these tools in the near future by systems biology approaches enhancing understanding of the ubiquitin-proteasome system from single protein degradation pathways to its influence on developmental processes.

Keywords: fluorescent protein; BFP; CFP; GFP; RFP; photoconvertible FP; fluorescent timer; tandem FP timer; proteasome; proteolysis; protein degradation; ubiquitin-proteasome system; ubiquitin; degron

1. Properties of fluorescent proteins used for protein degradation assays

The impact of the green fluorescent protein (GFP) and its derivatives on cell biology has been tremendous. These molecules have provided insights on the localization and dynamics of single proteins, complexes, and organelles in living cells. Furthermore, fluorescent proteins (FPs) with emission colors spanning the whole visible spectrum have been developed in the past decades to follow independent events simultaneously. The aim of this ongoing process is to develop bright,

monomeric, fast maturing, photostable FPs covering the full visible spectrum that are functional in all cellular compartments [1–3].

Although FPs are mostly used either as transcriptional reporters or to characterize the localization and/or dynamics of a specific protein, initial attempts to use GFP as a reporter in protein degradation assays began early on [4]. In this review, we will summarize the most common techniques in which FPs report protein degradation and highlight biophysical properties of FPs that are important for these assays. Initial studies used single FPs as readout for protein abundance. Later on, the methodology advanced to the usage of dual-color referencing, photoconvertible FPs, and fluorescent timers (FTs) to facilitate investigations. Researchers applied these more sophisticated degradation assays and proteome-wide screens to uncover whole protein degradation pathways by systems biology approaches. Regarding FTs, either specialized FPs that switch their color due to a second chromophore oxidation step or a tandem combination of a fast maturing FP with a slow maturing FP are used [5–7]. In both cases, ratiometric determination of fluorescence intensity reports the age of the whole fusion protein. Photoconvertible FPs are an alternative for *in vivo* pulse-chase experiments, as they allow for the labeling of an existing pool of proteins at a specific time point. Following this molecule pool over time is a convenient way to determine the stability of a protein. Moreover, *de novo* protein biosynthesis can be recorded after the photoconversion by the synthesis of unconverted FP molecules [8].

The biophysical features of the FP fused to the protein of interest (POI) could influence the characterization of protein stability. A critical feature in the context of protein degradation assays is the use of a monomeric FP in the fusion protein. The formation of dimers or tetramers, which were present in many older GFP and RFP variants, might lead to changes in a degradation pathway or the requirement of additional factors [9]. The maturation half-time of the FP is another characteristic with a huge impact on protein degradation assays. In the case that the maturation half-time of the FP is much longer than the half-life of the POI, most proteins in the degradation assay will be invisible to the observer due to FPs with non-matured chromophore [10]. If the two values are similar, about 50% of the POI will be undetected in the assay. Only if the maturation time is much shorter than the degradation half-life will most POIs be observable. Although this condition demands the usage of FPs with a short maturation time, FPs of distinct color with differences in maturation time are crucial for a novel type of reporter construct of protein age, the tandem FP timer [7].

The maturation time of an FP can also influence the data in other types of assays. In the case of a translational shut-off experiment, in which a translational inhibitor like cycloheximide is used to stop protein biosynthesis [4], maturation of the existing FPs continues for the duration of the experiment [11]. Consequently, the fraction of matured FPs increases over time. This ongoing maturation has to be considered in the interpretation of the experimental results if an FP with longer maturation time is used in an assay of relatively short time frame. Thus, not only the overall brightness, but also the maturation time of a given FP influences its successful application as a reporter in an assay. Therefore, the differences in biophysical properties of common FPs (**Table 1**) should be considered before constructs are generated.

Table 1. Biophysical properties of fluorescent proteins.

Protein	Excitation maximum (nm)	Emission maximum (nm)	Quantum yield	ε (extinction coefficient) (M^{-1} cm^{-1})	Molecular brightness (10^3 M^{-1} cm^{-1})	Oligomeric state	$\tau_{1/2}$ maturation 37 ℃ [min]	pKA	References	Used in
mTagBFP2	399	454	0.64	50600	32.38	monomer	12	2.7	[12]	[13]
tagBFP	402	457	0.63	52000	32.76	monomer	13	2.7	[14]	[15]
MTurquoise2	434	474	0.93	30000	27.9	monomer	33.5*	3.1	[10,16]	[17]
eCFP	434	477	0.4	32500	13.0	monomer	-	4.7	[18–21]	[22–25]
eGFP	488	507	0.6	55900	33.54	weak dimer	25	6.0	[26–29]	[7,15,23,24,30–42]
mEGFP	488	507	0.6	56000	33.6	monomer	14.5*	6.0	[43,44]	[15,35,38]
avGFP	395	509	0.79	25000	19.75	dimer	36.1*	4,5	[10,45–48]	[4]
Emerald	487	509	0.68	57500	39.1	weak dimer	11.2*	6.0	[10,20]	[15]
GFPm	503	509	0.42	84000	35.28	-	5.6	6.7	[49,50]	[35]
sfGFP	485	510	0.65	83300	54.15	monomer	13.6*	5.5	[10,51]	[7,25,35,52–62]
GFP (S65T)	490	510	0.64	55000	35.2	dimer	-	5.5	[48,63]	[64]
moxGFP	486	510	0.58	87000	50.46	monomer	17.1*	-	[10,65]	[15]
sGFP	495	512	0.62	42000	26.04	monomer	-	6.0	[66]	[33]
GFPmut3	500	513	0.39	89400	34.87	monomer	4.1	-	[10,26]	[67]
mNeonGreen	506	517	0.8	116000	92.8	monomer	10.9*	5.7	[10,68,69]	[33,35]
mGFP A206K	-	-	-	-	-	-	-	-	[15]	[15]
GFPmut3 V206R	-	-	-	-	-	-	-	-	[35]	[35]
GFP S65C	-	-	-	-	-	-	-	-	[37]	[37]
mCitrine	513	527	0.74	94000	69.56	monomer	-	5.6	[70–72]	[24]
eYFP	513	527	0.67	67000	44.89	weak dimer	9*	6.9	[10,73–75]	[76,77]
Venus	515	528	0.57	92200	52.55	weak dimer	17.6*	6.0	[10,78]	[13,15,17,22,60]
Citrine	516	529	0.76	77000	58.52	weak dimer	-	5.7	[19,70]	[79]
mOrange2	549	565	0.6	58000	34.8	monomer	270	6.5	[43]	[55]

Continued on next page

Protein	Excitation maximum (nm)	Emission maximum (nm)	Quantum yield	ε (extinction coefficient) (M^{-1} cm^{-1})	Molecular brightness (10^3 M^{-1} cm^{-1})	Oligomeric state	$\tau_{1/2}$ maturation 37 ℃ [min]	pKA	References	Used in
tdTomato	554	581	0.69	138000	95	dimer	60	4.7	[43,80]	[15,52]
DsRed	558	583	0.79	75000	5.17	tetramer	600	4.7	[43,80]	[7,31,32,34,37,42]
tagRFP	555	584	0.48	100000	48	monomer	42	3.1	[10,43,81]	[15,39,52,82]
DsRed-Express2	554	591	0.42	35600	14.95	tetramer	42	-	[83]	[58]
mScarlet-I	569	593	0.54	104000	56.16	monomer	25.7*	5.4	[10,84]	[54]
mScarlet	569	594	0.7	100000	70	monomer	132.4*	5.3	[10,84]	[13]
mRFP1	584	607	0.25	50000	12.5	monomer	21.9*	4.5	[10,43,80,85]	[38,57,64]
mCherry	587	610	0.22	72000	16	monomer	15	<4.5	[43,80]	[7,15,23,25,35,38,52–54,56,58,60–62,67]
mKate2	588	633	0.4	62500	25	monomer	34.4*	5.4	[10,86]	[17,52]
mKate	588	635	0.33	45000	14.85	monomer	75	6.2	[87]	[23–25]
iRFP	690	713	0.06	105000	6.3	dimer	168	4.0	[88]	[76]
fmCherry	-	-	-	-	-	-	6		[52]	[52]

*Maturation time taken from [6]

A diverse array of protein degradation assays have been developed based on single FPs as well as their combinations [3], convertible FPs [89], and timers [5–7]. Next, we will give a short introduction into protein degradation followed by an overview of the different techniques used to monitor protein degradation and to critical biophysical properties of FPs that are important for these applications.

2. Protein degradation by the ubiquitin proteasome system

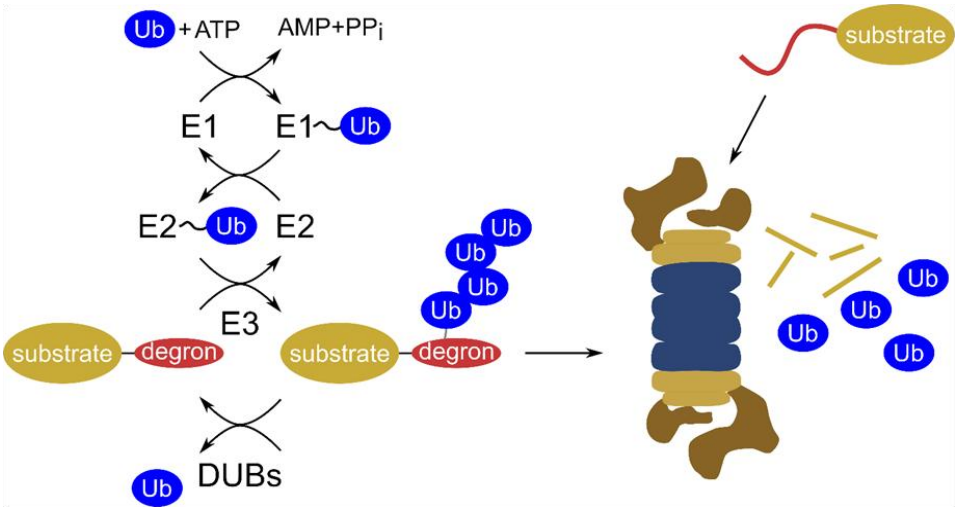

Figure 1. Protein degradation by ubiquitin-proteasome system. Protein degradation by the proteasome uses two pathways. The vast majority of proteins are degraded via a ubiquitin-dependent mechanism. Here, a substrate is ubiquitylated by an enzymatic cascade consisting of an E1 (ubiquitin-activating enzyme), an E2 (ubiquitin-conjugating enzyme), and an E3 (ubiquitin-protein ligase). The E3 recognizes the substrate at a degradation sequence (degron) that is sufficient to confer degradation and is transferable. The ubiquitylated substrate is recognized by the proteasome; proteolysis takes place in the interior of the complex. Ubiquitin is removed from the substrate during degradation by a deubiquitylating enzyme (DUB). More DUBs are present in the cell elsewhere, which can lead to the complete removal of ubiquitin moieties from a substrate or shaping of a ubiquitin chain prior to proteasomal engagement. A second proteolysis pathway is ubiquitin-independent. This requires direct recognition of a degron by the proteasome. Proteolysis in the interior of the proteasome proceeds in the same way as for ubiquitin-dependent degradation.

Regulated protein turnover plays important roles in eukaryotic cells, allowing them to shape their proteome in accordance to extracellular and intracellular signals and serving as a basic mechanism to ensure cellular viability. Deregulation of protein turnover or defects in proteolysis are connected to severe diseases as well as cellular and organismic aging in higher eukaryotes [90]. The characterization of basic degradation pathways as well as determinants of protein stability is therefore of high importance. In eukaryotes, one of the main machinery for regulated protein turnover is the ubiquitin-proteasome system (UPS; **Figure 1**). The small protein ubiquitin is a tag that can mark proteins for degradation by a protease complex, the so called proteasome [91,92]. In brief, ubiquitin is activated by the ubiquitin-activating enzyme (E1) through adduct formation of the C-terminal glycine of ubiquitin with a cysteine in the E1 in an energy-rich thioester bond. Transesterification onto a cysteine in a ubiquitin-conjugating enzyme (E2) primes the activated ubiquitin for the transfer onto the substrate. In general, an E2 forms a complex with a

ubiquitin-protein ligase (E3) that selects the substrate. Substrate binding by the E3 stimulates the transfer of ubiquitin to the substrate; usually, it is fused covalently to the ε-amino group of a lysine. This step may be repeated further through the addition of ubiquitin moieties to a ubiquitin already attached to the substrate, resulting in the formation of polyubiquitin chains. This elongation sometimes requires the action of a fourth enzyme (E4) for efficient ubiquitin chain formation. Moreover, several different mechanisms of ubiquitin transfer have been identified by biochemical studies. Excellent reviews provide detailed information about the basic mechanism of protein ubiquitylation [91–94].

In general, proteasomal proteolysis requires a chain of at least four ubiquitin moieties linked to each other via the C-terminus of a ubiquitin fused to a lysine at residue 48 in the previous ubiquitin or ultimately in the substrate [95]. Although such a linear ubiquitin chain is sufficient to target a ubiquitylated protein for degradation, the *in vivo* situation is more complex. Ubiquitin has seven lysines as well as the N-terminus for further ubiquitylation, which enables a variety of linear chains or branched complexes with diverse patterns as substrate ubiquitylation outcomes. Ultimately, the ubiquitylation pattern influences the fate of the modified protein, with linear chains linked through K11 or K48 signaling for proteasomal degradation [96,97].

The polyubiquitin chain is recognized by subunits in the regulatory particle of the proteasome or by adapter proteins that bind to the polyubiquitin chain and to the regulatory particle. Substrate unfolding by AAA-ATPases requires an unfolded sequence stretch. Concomitantly, the substrate is transferred to the inner cavity of the proteasome where the proteolysis into peptides takes place. The polyubiquitin chain is removed from the substrate before or during degradation by a deubiquitylating enzyme and recycled for further rounds of ubiquitylation [98].

Substrate selection occurs mostly by E3s that recognize degradation sequences (degrons) in the substrate. A degron is defined as a part of a protein that is necessary and sufficient for degradation [99,100]. In the context of the UPS, degrons are often short, transferable sequence motifs that are bound by an E3, which induces ubiquitylation and degradation. Thus, degrons typically contain several distinct features: a recognition motif for the E3, at least one lysine for the attachment of a polyubiquitin chain and a stretch of unfolded amino acids for the induction of proteasomal proteolysis [101]. Some specialized degrons are not bound by an E3 and do not require polyubiquitylation to induce proteasomal degradation. Instead, these degrons bind directly to the regulatory particle of the proteasome and induce proteolysis of the substrate. However, an unfolded region of sufficient length is still required in the substrate to allow unfolding and degradation of the protein. The best-studied example following this kind of degradation mechanism is the so-called cODC degron, derived from the carboxy terminus of murine ornithine decarboxylase (ODC). The degradation of cODC by the proteasome via this mechanism is conserved between diverse eukaryotes, as the degradation-inducing function of cODC has been observed in mammalian, plant, insect, and yeast cells [102,103].

The mode of substrate selection, by an E3 or by the proteasome itself, cannot always be easily distinguished. Some substrates simply follow both routes like the well-studied transcription factor Rpn4 [104,105]. Depending on the molecular or cellular environment, gradual changes in degradation route are possible. One example is the photosensitive degron (psd) module, an optogenetic tool for light-induced protein degradation that is useful for generating conditional mutants of essential proteins in yeast [39,82,106]. For activation of the psd module, a synthetic variant of the proteasome-recognized degron cODC becomes exposed following light-triggered

structural changes of a photoreceptor. Whereas soluble psd-modified proteins seem to be mostly recognized directly by the proteasome, with only a minor fraction of the activated psd dependent on the E3 Doa10 for degradation, ER membrane proteins fused to psd are completely dependent on Doa10 for degradation [107]. Although the proteasome is active close to the ER membrane [108,109], it does not seem to recognize the cODC degron of psd close to the membrane. These findings exemplify the necessity of mapping degradation pathways in detail and indicate a lack of knowledge concerning the recognition of substrates by components of the UPS.

FPs are excellent reporter proteins to test degrons and the different features of a degron, as they can be easily observed in living cells. Their natural stability against proteolysis makes them almost ideal reporters to investigate proteolysis and presents the possibility of identifying whole degradation pathways in large scale [42]. Non-FP based compounds have been employed to study the UPS as well, which have been reviewed elsewhere [110–113].

3. Fluorescence reporters for the observation of protein kinetics

Diverse strategies have been used to follow protein degradation in eukaryotes with FPs. Common observation techniques for FPs were used, namely quantitative fluorescence microscopy, fluorescence detection by plate reader, and flow cytometry. Not surprisingly, the first applications in protein degradation relied on GFP as a reporter.

3.1. Fusion with a conventional FP

Historically, the usage of GFP in living cells and as a marker for protein localization was soon followed by application as a readout for protein degradation events [4,114,115]. Subsequently, fusions of GFP to proteins of interest and random mutagenesis were used to identify genes involved in turnover of the target in budding yeast [116,117]. Similar approaches have also been undertaken in mammalian cells, either to identify degradation enhancing sequences or to study protein degradation on single cell level. An early investigation aimed at identifying novel degron sequences in mammalian cells used GFP as reporter and detection by flow cytometry [118]. Protein synthesis was stopped by the translational inhibitor cycloheximide, which is one of the classical techniques for determining protein half-lives (**Figure 2A**) [119].

Apart from the search for new degrons and degradation pathways, the usage of destabilized eGFP or other FPs coupled to the cODC degron as well as the application of reporter substrates like Ub^{G76V}-GFP as transcriptional reporter is widespread for investigating UPS activity or screening for proteasome inhibitors [120]. Quantification of the POI is usually achieved by fluorescence microscopy or flow cytometry and fluorescent reporters have been detected in single cells, living microarray format, or whole animals [41,121–130]. A combination of automated high-throughput microscopy with a translational shut-off by cycloheximide was used to characterize protein degradation kinetics and cell-to-cell variations of destabilized eGFP in a large number of mouse fibroblast cells. [30,41,131]. One problematic aspect is that quantification of a single FP fused to the POI is affected by cell-to-cell differences in expression [132], which might influence the interpretation of the results.

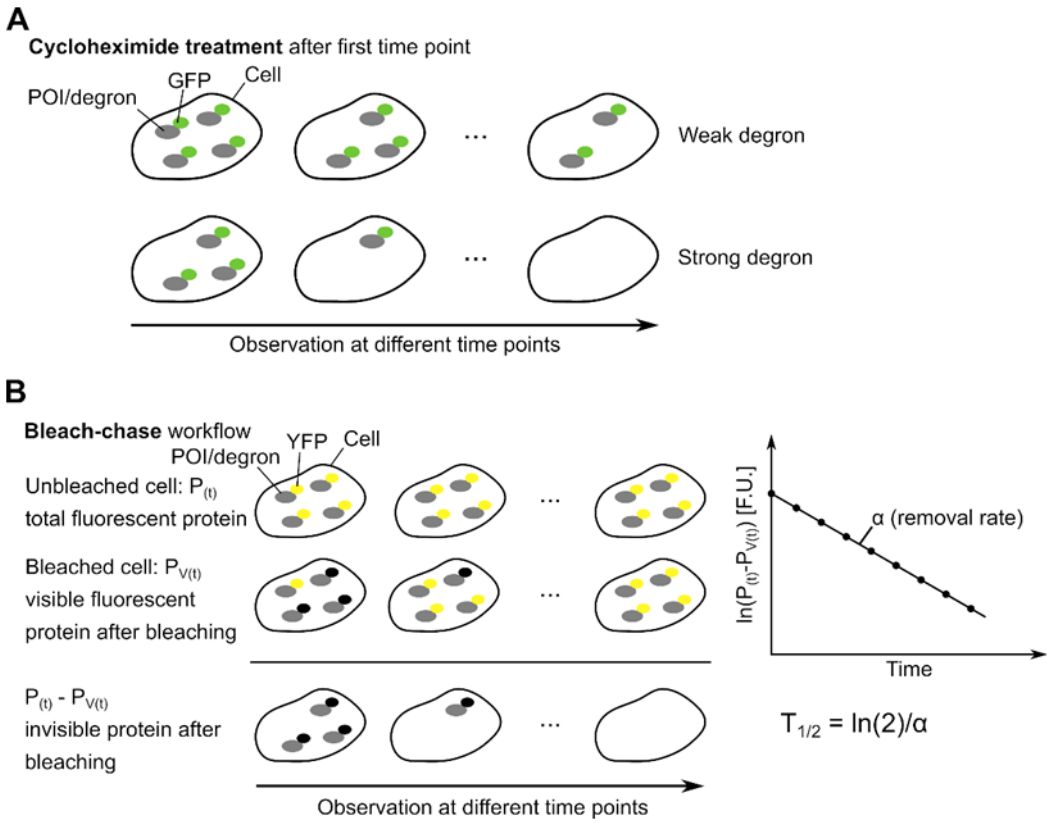

Figure 2. Measurement of protein half-lives with an FP fused to the protein of interest. A) GFP-dependent measurement of protein degradation with a cycloheximide chase assay. A protein of interest (POI) containing a degron or an isolated degradation sequence is fused to GFP. Depending on the strength of the degron or the rate of protein turnover, weaker or stronger fluorescence will be measurable at the beginning of the experiment. Addition of the translational inhibitor cycloheximide will lead to a stop in protein synthesis and subsequent decay of the fluorescence signal depending on the strength of the degron. Time-lapse analysis of GFP fluorescence results in characterization of the protein half-life. B) The bleach-chase requires observation of protein abundance over time in undisturbed (P) and bleached cells (P_V). It is sufficient to bleach a fraction of the molecules in the bleached cells. Re-establishment of fluorescence to similar levels as the unbleached cells depends on the removal rate (α), which depends on the degradation rate of the POI and the dilution by cell divisions. The fraction of bleached molecules is calculated from the difference in signal intensity of bleached and unbleached cells. The half-life ($T_{½}$=ln(2)/α) is obtained by semi-logarithmic plotting of the difference between the value for the unbleached and bleached cells. The protein removal rate α is the slope of the decay over time.

Further applications of FPs as degradation reporters comprise characterization of known degrons and the search for novel ones. Usually, the implementation and quantification is performed in a similar way as pioneered by Hampton *et al*. 1996 [4]. However, combinations of FPs have also been used to track the abundance of the degron fused to an FP and to follow the expression of a protease simultaneously observing proteolytic cleavage of a substrate with concomitant degron

activation [23,24]. In microorganisms like budding yeast, FPs are directly observable in colonies and cell lawns [82,116]. Detection of the fluorescence level allows one to screen for novel components of a degradation pathway or to search for degron variants with higher activity [39,117]. Moreover, characterization of protein degradation at single cell level, the characterization of natural degrons, and the development of synthetic degrons relies heavily on the usage of FPs [13,17,38,40,76,133]. Often, degrons are readily transferable between eukaryotes, due to the high conservation of the UPS [91,103]. Depending on the cellular context, however, surprising effects have also been observed. One example is degrons that induce protein degradation in yeast or in mammalian cells, but lead to protein aggregation in *Caenorhabditis elegans* [37,134,135]. In *C. elegans*, these sequences are not acting as specific proteasome-targeting signals. Instead, they alter the structure of the GFP resulting in aggregation-prone proteins that are recognized by the chaperone system. Overloading the capacity of chaperone-based degradation pathways then leads to the formation of toxic aggregates [37].

Localization of fully active proteasomes has been detected with bifunctional molecules. These molecules form a covalent bond to a threonine residue in the active center of a proteasome subunit and have a fluorophore attached to themselves by a linker [136]. Although mostly non-FP-based fluorescent compounds have been used for this purpose, it is a neat addition to the toolbox for visualizing localization of proteasomes engaged in protein degradation.

The usage of FPs in living cells is not always without obstacles, especially in cases where absolute or relative amounts of protein levels must be correlated with fluorescence intensities. Common challenges include the transfection efficiency of the reporter construct, which depends on cell type and size of the plasmid/construct. This influences how many cells in the assay are carrying the reporter and lead to variations in expression strength [137–140]. Although these factors do not influence the half-life of a reporter, they have an impact on fluorescence quantification. Below, we describe some methods that were developed to address some of these challenges, for example imaging of two cell lines together, usage of a photoconvertible FP, ratiometric reporters, or usage of tandem FP timers.

One characteristic of cells is that they exhibit fluorescence of metabolites and compounds of their own [141–143]. This autofluorescence signal will add to the signal of the FP and must be taken into account for quantification of the specific signal. Usually, compensation requires measurement of cells without the FP.

The bleach chase is a remarkable method relying only on single modification of the POI with one fluorophore (**Figure 2B**). Here, time-lapse analysis of undisturbed cells versus cells in which the FP has been bleached is used to calculate the protein removal rate [77]. Application requires a microscope that allows bleaching of the FP in selected cells, which is usually achieved by a laser. One should use a bright FP with relatively low photostability to minimize phototoxic effects during bleaching, but photostable enough to allow long-term observation of the cells. A fast-maturing FP is critical to avoid distortions when calculating the invisible molecule fractions. Other critical parameters for obtaining meaningful results include quantification of the autofluorescence and bleaching of the fluorophores during long-term observation of the cells.

In one study, a network implementation was used to obtain direct visualization of UPS activity. The genes of stable FPs were integrated into a genetic circuit with a destabilized transcriptional activator to link proteasomal activity with transcription of a fluorescent reporter. Thus, long-term investigation of proteasomal degradation and UPS activity is facilitated in mammalian cells [144].

The usage of fluorescence microscopy in protein degradation assays in order to identify novel

degradation pathways in high throughput screens proves challenging due to the relatively low image acquisition speed and the need for proper image segmentation and fluorescence intensity quantification. Nevertheless, microscope automation has been used to circumvent these obstacles. In a high throughput microscopy-based search for targets of the E3 Grr1 in yeast, staining of yeast cells with a dye enabled cell detection. Yeast POIs were labelled with GFP and Grr1-dependent degradation was monitored in a mix of two cell lines for each GFP-marked POI, one with endogenous Grr1 and one lacking Grr1 that was labelled by RFP. Both cell lines were imaged simultaneously, positive hits were identified by high abundant GFP fluorescence in RFP-containing cells [64]. Thus, side-by-side comparison of cells with and without operational Grr1 was used to identify POIs degraded via the E3 Grr1. This method circumvented the necessity for precise quantification of the POI, which could be affected by fluctuations in fluorescence intensities. Usage of FPs as reporters is a very common technique; however, the last example of high-throughput screening also exemplifies the problems that one has to face: cell-to-cell variations in fluorescence that are invoked by extrinsic and intrinsic factors [132]. Coupled with fluctuations in fluorescence detection, these variations impede the elucidation of protein degradation pathways. In the search for Grr1 substrates, simultaneous detection of cells with and without Grr1 was used to minimize this problem. Another possible solution is using a reference fluorophore that normalizes the fluorescence to an internal control.

3.2. *Conversion of fluorescent proteins*

The development of photoconvertible FPs facilitated characterization of protein dynamics, among them also protein degradation. Photoconvertible FPs change their fluorescence color in response to irradiation with light of a specific wavelength like Dendra2 or switch from non-fluorescent proteins to fluorescent ones like PA-GFP (photoactivatable GFP). Some examples are given in **Table 2**.

Table 2. Selected photoconvertible and photoactivatable fluorescent proteins.

Protein	Excitation maximum (nm)	Emission maximum (nm)	Quantum yield	ε (M^{-1} cm^{-1})	Molecular brightness (10^3 M^{-1} cm^{-1})	Oligomeric state	pKa	Publication	Used in
Dendra2 (green)	490	507	0.5	45000	22.5	monomer	6.6	[145–148]	[8,79,149]
Dendra2 (red)	533	573	0.55	35000	19.25	monomer	6.9	[145–148]	[8,79,149]
PA-GFP [on]	504	517	0.79	17400	13.75	monomer	-	[150]	[76]

After photoconversion, the decrease in the specific fluorescence signal, which depends on the degradation rate, can be measured without the use of inhibitors of protein biosynthesis (**Figure 3**). Photoconvertible FPs have proven useful for monitoring real time protein degradation on a single-cell level and have shown potential for high throughput analysis [8,151]. The green-to-red photoconvertible FP Dendra2 was successfully used to determine different degron-mediated protein

half-lives in cultured cells [8] as well as for the measurement of UPS activity dependent on cell-type and age in *C. elegans* [149]. Moreover, photoconvertible FPs were used in cultured cells as well as in *Drosophila*, mouse, and zebrafish embryos to measure protein turnover dynamics [152–155].

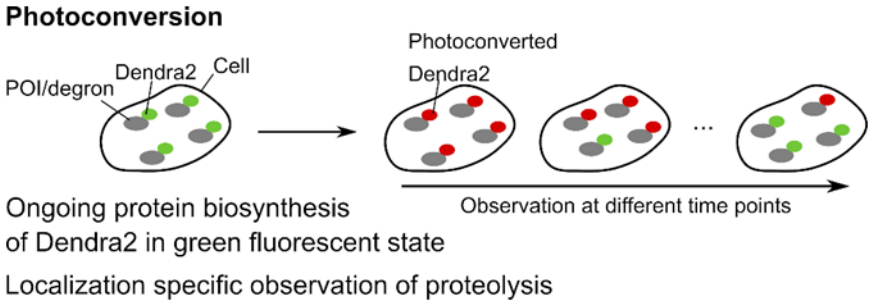

Figure 3. Characterization of protein half-life with the photoconvertible FP Dendra2. Dendra2 is fused to the protein or degron of interest and expressed in the cell line of choice. Photoconversion from green to red takes place by exposure of Dendra2 to UV or blue-light. Thus, red fluorescence labels the POI that are present in the cell at the time of photoconversion. Tracking of these molecules over time is a convenient method to obtain the protein half-life. Ongoing protein synthesis results in the generation of Dendra2 in the green fluorescent state.

Similar to the usage of a single FP as degradation reporter, measurements are affected by cell-to-cell variations in protein expression. However, in comparison to conventional FPs, photoconversion has the clear advantage that autofluorescence of individual cells can be measured before photoconversion. This leads to more reliable measurements of the degradation of the POI. In order to ensure that a large fraction of the molecules in a cell are highlighted during the assay, the photoconvertible FP should ideally exhibit high brightness in the converted state and fast maturation into the non-converted state. Unfortunately, most photoconvertible FPs are less bright than conventional FPs and maturation times to the non-converted fluorescent state are not always available. Complete photoconversion of all molecules in a cell is not necessary to measure the degradation rate. For most proteins, the intracellular decay rate follows first order kinetics and is independent from the amount of molecules present at the beginning [156–158]. Nonetheless, the better the photoconversion rate, the better is the signal to noise ratio, which facilitates quantification of the converted FP signal.

A variation of FP conversion is the recombination-induced tag exchange (RITE), which relies on a genetic switch in the FP fused to the protein of interest by the Cre recombinase. Here, the Cre recombinase removes a sequence stretch containing a GFP gene as well as a selection marker in order to bring an RFP gene in frame with the gene of interest [159]. Thus, the protein of interest is synthesized before the Cre switch with GFP and afterwards all newly synthesized molecules are fused to RFP. Time-lapse recording coupled with quantification of GFP and RFP signals before and after the switch achieves monitoring of protein turnover as well as biosynthesis of the protein of interest (**Figure 4**). FPs with fast maturation times are important in order to avoid distortion of the degradation measurement and delay in observation of the newly synthesized molecules after switching.

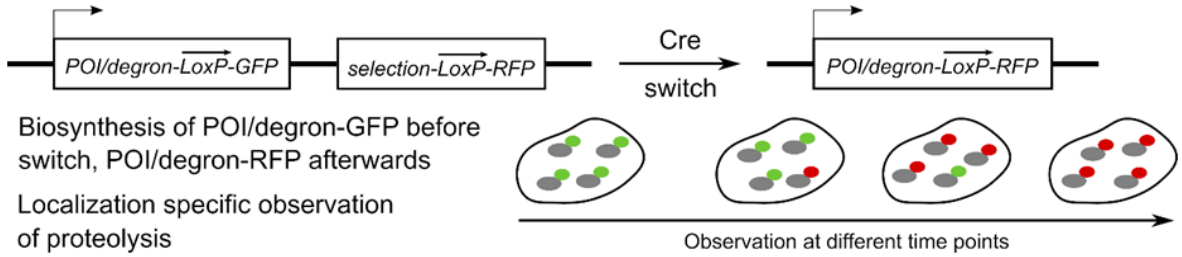

Figure 4. Genetic FP conversion with the Cre recombinase using the recombination-induced tag exchange (RITE) method. The protein or degron of choice is fused with a LoxP-GFP-selection marker-LoxP-RFP cassette on DNA level (LoxP-sequences with the same directionality). Before switching, a GFP tagged construct is expressed. Cre expression leads to the removal of the GFP and the selection marker part, which results in an RFP tagged construct. Observation of the GFP fluorescence over time after initiation of the switch allows measuring the half-life of the protein or degron of interest and the appearance of the RFP fluorescence reports about the expression strength.

RITE has been applied in mammalian cell culture to investigate cell cycle dependence and cell to cell variation of proteasomal proteolysis, degradation of nuclear inner membrane proteins, and long-lived proteins in postmitotic cells [55,160,161]. In budding yeast, the method has been used to investigate the distribution of proteasomes in aged and starving cells, destruction of mitochondria in aged cells, and the behavior of long-lived proteins [162–164].

3.3. Ratiometric reporter using a second fluorescent protein

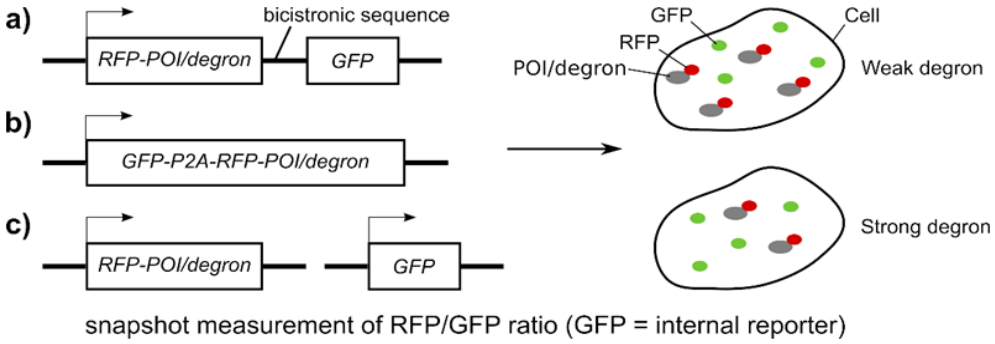

Figure 5. Ratiometric measurement of protein abundance with an internal reporter using snap-shot measurements of protein abundance. An FP (RFP in this example) is fused to the protein or degron of interest. Another FP (here: GFP) is produced via bicistronic expression using an IRES sequence (a) or a viral 2A linker (b) or another promoter (c). In all cases, the stable GFP is produced in a fixed relation to the RFP containing construct. Quantification of the RFP/GFP ratio by steady state snap-shot measurements reports about the abundance of POI abundance without interference of cell-to-cell variations in protein biosynthesis. Thus, stability of the protein or degron of interest can be easily compared across different conditions, e.g. in presence or absence of UPS components to elucidate a degradation pathway.

Another approach to characterizing protein degradation is to monitor the fluorescence intensity ratio of two different FPs. This system uses two FPs that are translated from a bicistronic mRNA. Separation of the coupled proteins at translation level in eukaryotes can be achieved by inserting different sequences between the two genes. For example, an internal ribosomal entry sequence (IRES), a viral 2A-peptide sequence, or two constitutive promoters have been used for the fluorescence-based characterization of protein stability in mammalian and yeast cells (**Figure 5**) [25,31,58].

In relation to the IRES or the 2A-peptide sequence, expression levels will not necessarily be the same, but a fixed ratio will be achieved. One FP acts as an internal reporter, whereas the other one is fused to the POI. Changes in the fluorescence intensity ratio of both proteins are correlated to the degradation of the POI and are not altered by fluctuations in transcription or translation. Thus, ratiometric measurements enable snap-shot measurements that facilitate screening of many POIs in a short time. Proteome-wide association studies to decipher degradation pathways are feasible with this approach. Important features of the FPs include fast maturation of both FPs in order to ensure correct calculation of the ratio.

Such a bicistronic approach based on IRES combined with the hORFeome proteome library, microarray technique and fluorescent-activated cell sorting enabled the investigation of a larger set of proteins in mammalian cells. This so-called fluorescence-based global protein stability (GPS) profiling is a systematic, high throughput approach to monitor protein turn over, which allows the observation of dynamic changes in protein stability dependent from stimuli or genetic manipulation. For GPS profiling and identification of substrates of the Skp, Cullin, F-box containing complex (SCF) in cultured cells, the FP DsRed was used as an internal reporter and an eGFP was fused to the POI. Bicistronic expression was obtained by using an IRES sequence placed between the RFP and the GFP construct [31,32,42]. In addition, this methodology has been successfully used to screen for C-degrons in mammalian cells [34,165] and to develop a system for induced protein degradation using proteasome adaptors in mammalian cells [166].

It should be taken into account that the existing mechanisms to generate bicistronic mRNAs in eukaryotes have certain imperfections. A reduced expression efficiency of the downstream open reading frame (orf) has been observed for IRES sequences [167]. This behavior can be minimized with IRES sequences that mediate different expression rates of the downstream orf and repetition of certain IRES sequences [168–171]. In addition, the types of orfs flanking the IRES sequence as well as the length and secondary structure of the non-coding inter cistronic sequence between the orfs influence the expression rate [172,173]. Despite these issues, it has been successfully implemented to obtain large-scale information about protein degradation pathways in mammalian cells.

Another ratiometric method was used to compare efficiencies of degron-module variations in yeast. Here, super-folder GFP (sfGFP) was used as reference and mCherry as reporter that was destabilized by fusion to various degron-modules. Bicistronic expression was achieved by an insertion of a viral 2A-peptide sequence [25]. The viral 2A-peptide sequence causes ribosomal skipping during translation, which results in two separated proteins [174]. Nonetheless, it has been observed that these sequences do not always result in complete separation of both proteins and that the production of the second protein is reduced [175]. There are different 2A-peptide sequences with varying cleavage efficiencies that also depend on the used cell type as well as an optimization strategy via modification of the 2A codons [174,176]. Despite these issues, the method has been used to compare protein stabilities and to monitor dynamic changes invoked by external factors [25,177–180].

A third approach was used to compare the strength of commonly used degrons in

Saccharomyces cerevisiae. In this case, the RFP DsRed was expressed as reference from a constitutive promoter and a YFP fused with the different degrons from another promoter. Quantification of degron strength was achieved by ratiometric snap-shot measurements [58]. This technique was also used to investigate the importance of disordered regions and ubiquitin-like domains in proteasomal proteolysis [181]. Overall, the diverse examples of successful usage of internal controls demonstrate the robustness of this approach. The viral 2A and IRES sequences promise small and compact constructs at the expense of non-fully separated constructs or unequal production of the POI compared to the internal control. In contrast, usage of two expression cassettes results in considerably larger constructs and equal expression of reporter and degron construct depends on the promoters in use.

3.4. Fluorescent timers

The tandem fluorescent timer (tFT) consists of two FPs with distinct maturation rates fused to a POI. In most implementations, the fast maturing sfGFP (maturation half-time: 6 min) is coupled to the slower maturing mCherry (two step maturation: 17 min and 30 min) [7]. Thus, a POI is marked by the sfGFP and its average age can be deduced by the maturation state of mCherry in relation to the fluorescence intensity of the GFP (**Figure 6**).

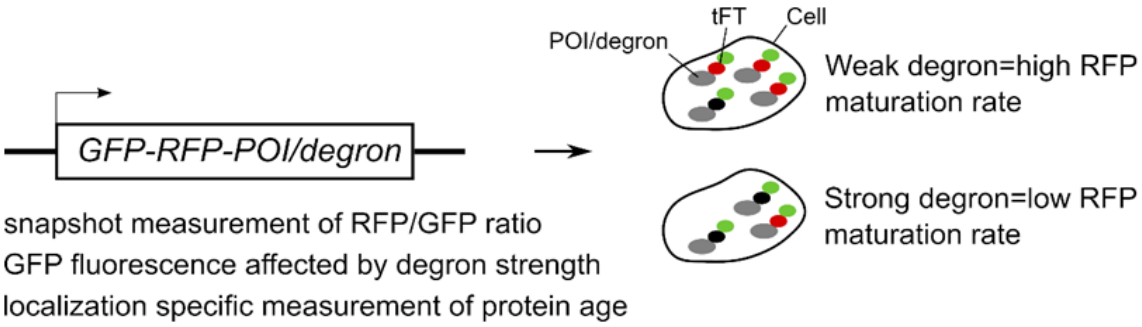

Figure 6: Ratiometric measurement of degron activity by tandem FP timer (tFT) with snap-shot imaging. A GFP-RFP tandem FP tag is fused to the protein or degron of interest with the GFP distal to the protein/degron. Maturation of RFP is slower compared to the GFP, thus the RFP/GFP ratio reports on the age of the fusion protein. A lower RFP/GFP ratio indicates a "younger" protein with higher turnover, a higher RFP/GFP ratio an "older" protein with lower turnover. Thus, the degradation rate can be deduced from snap-shot measurements. Comparison of measurements done in the presence or absence of UPS components allows characterization of degradation pathways. Usage of RFP variants with different maturation times in the tFT allows tuning of the observable spectrum of half-lives.

Shortly after protein biosynthesis, the fusion protein will show only green fluorescence, due to the fast maturation rate of sfGFP, resulting in a low mCherry/sfGFP intensity ratio. Over time, the slower maturing mCherry becomes fluorescent and the ratio increases with protein age. POIs with a fast turnover will have a very low mCherry/sfGFP fluorescence ratio, as the POI is degraded before mCherry maturation is complete. Proteins with slower turnover rates will have a higher ratio due to

the increased number of molecules with matured mCherry. As only snap-shot measurements are necessary to characterize the age of a POI, proteome wide investigation of protein turnover is easily achieved with libraries of tFT-tagged proteins. Different time ranges can be achieved through coupling FPs with different maturation times together [7,35]. One of the FPs should always have a fast maturation time. Changes in the FP with slower maturation kinetics adapts the tFT to match the characteristics of the process of interest. By measuring the fluorescence intensities and calculating the mCherry/sfGFP intensity ratio, it is possible to determine protein kinetics, spatio-temporal localizations, and protein degradation kinetics with tFTs. Importantly, the tFT is fused to the POI in a way that the GFP is placed distal to the degradation site, as sfGFP is known to be incompletely degraded by the proteasome [35]. However it should be noted that the maturation times can also be influenced by different cellular conditions or the cellular localization [7].

The tFT assay was used in yeast to assay the stability of POIs in dependence to o-glycosylation, to reveal the degradation pathway of mitochondrial membrane proteins, and to investigate protein degradation of mislocalized tail-anchored membrane proteins [53,54,62]. Pooled libraries of tFT tagged proteins containing different N-terminal sequences were used to study N-terminal degrons in single cells with fluorescence–activated cell sorting analysis [61]. In addition, the tFTs were successfully utilized in yeast to investigate the turnover rates of several putative targets of the inner nuclear membrane-associated degradation (INMAD) Asi complex and the endoplasmic reticulum associated protein degradation (ERAD) system [60]. Moreover, a tandem FP timer with sfGFP coupled to mOrange was used to study cell cycle dependence of proteasomal degradation as well as cell-to-cell variation of proteolysis in mammalian cells [55]. Here, it was shown that time-lapse recordings can be used to reveal changes in degradation and biosynthesis rate of a POI. The system was also applied in plants (*Nicotiana benthamiana* & *Arabidopsis thaliana)*, demonstrating its value to characterize protein half-lives in different genetic backgrounds via live cell imaging [56].

The utility of the tFT approach was also demonstrated in animals. Dona *et al*. used tFT-tagged G-protein coupled receptors to investigate their turnover rate as well as to track the signal transduction of cytokines in migrating cells in Zebra fish embryos [59]. In *Drosophila*, the tandem fluorescence timer was adapted to investigate the precise manner of bicoid gradient formation in embryos, highlighting the role of protein degradation in embryo morphogenesis [52].

The diverse applications of the tFT method, the usability in single cells or whole animals, and the possibility to infer the age of a protein, solely by snap-shot imaging argues for the importance of this method. As the age of a protein is directly related to its degradation rate, simple measurements are enough to assess protein stability at a given time point. Time-lapse recordings of tFTs incorporate information like changes in degradation and biosynthesis rates. Comparison of such data in whole animals or developing embryos multiplies the applicability and demonstrates the valence of this approach.

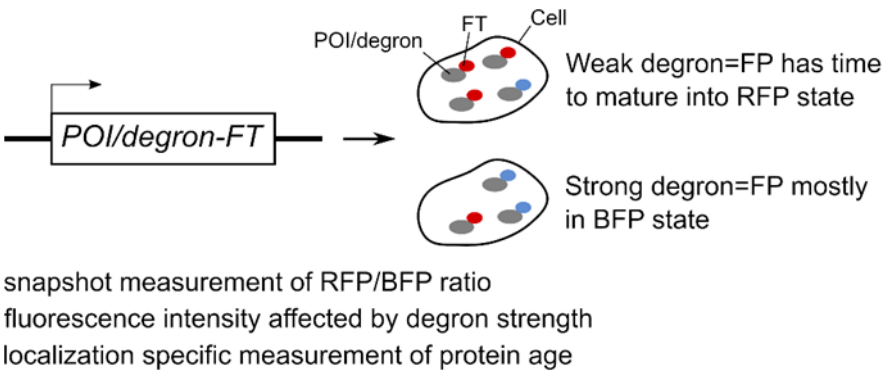

Figure 7. Ratiometric measurement of degron activity with fluorescent timers (FTs) by snap-shots. In the timer FPs, a monomeric FP matures via blue-fluorescence to an RFP. Different timers with different maturation times for the blue and red form exist (Fast-FT, Medium-FT, Slow-FT). The selected FT is fused to the protein or degron of interest. The "age" of the fusion protein decides if the FT is in the blue form ("young" fusion protein) or fully matured to the red fusion protein ("old" protein). The degradation rate can be deduced from snap-shot measurements and blue-to-red ratios. Investigations of degradation pathways are done by observations in the presence or absence of UPS components.

Table 3. Fluorescent protein timers.

Protein	Excitation maximum (nm)	Emission maximum (nm)	Quantum yield	Extinction coefficient ($M^{-1}cm^{-1}$)	ε (M^{-1} cm^{-1})	Oligomeric state	Characteristic times* 37 ℃ [min]	pKa	Publication
FAST-FT (blue)	403	466	0.3	49700	15	monomer	15	2.8	[6,36,79,182]
FAST-FT (red)	583	606	0.09	75300	7	monomer	426	4.1	[6,36,79,182]
Medium-FT (blue)	401	464	0.41	44800	18.4	monomer	72	2.7	[6,36,79,182]
Medium-FT (red)	579	600	0.08	73100	5.8	monomer	234	4.7	[6,36,79,182]
Slow-FT (blue)	402	465	0.35	33400	11.7	monomer	588	2.6	[6,36,79,182]
Slow-FT (red)	583	604	0.05	84200	4.21	monomer	1680	4.6	[6,36,79,182]

*Characteristic times corresponds to fluorescence maxima for the blue form and to maturation half-time for the red form

Recently, single FP timers have been described that show a blue-to-red fluorescence conversion [6]

(**Figure 7, Table 3**). They have been applied in mammalian cells to study proteasomal proteolysis, endosomal protein degradation and to generate a degron toolbox [36,79,182]. Although these timers are relatively slow in changing their fluorescence, the maturation time seems to be suited to follow proteolysis of certain events in mammalian cells. Tailored FPs like these timers with high brightness and different switching times might be a fruitful direction for further developments. The possible application range is similar to that of tFTs.

4. Concluding remarks

Usage of FPs to study protein degradation has resulted in characterization of numerous degradation pathways and the diverse fluorescence-based methods are valuable additions to the toolbox for investigating UPS-dependent protein degradation [42,113]. Yet, certain features of FPs have to be taken into account. One issue is the intrinsic stability of the β-barrel fold of FPs. It has been noted with different types of proteasomal substrates and in different organisms that an FP destined for degradation and already engaged by a proteasome might escape its fate [33,35]. The tight folding of the β-barrel might exceed the unfolding capability of the proteasome sometimes and a certain percentage of FPs escapes the degradation process. Moreover, the FP is released from the proteasome devoid of the degron sequence in this case, which protects it from further degradation attempts in the future. Thus, kinetic measurements relying solely on fluorescent measurements might be slightly shifted due to the presence of escaped FPs that accumulate over time. Especially K63-linked ubiquitin chains were found to be inefficient for proteasomal degradation of GFP [33,183].

However, not only the type of ubiquitylation is critical for efficient proteolysis of an FP, but also the stability of the β-barrel and the type of FP, e.g. sfGFP resists proteasomal degradation considerably whereas neonGreen is degraded more efficiently [35]. In bacteria, a stepwise unfolding of sfGFP has been suggested for the degradation by the ClpXP protease, which might indicate that partially digested proteins are able to escape the protease in-between the unfolding steps [184]. In line with such a view, changing the starting point for unfolding and proteolysis of the β-barrel by circular permutation has been demonstrated to minimize inefficient proteolysis of sfGFP by ClpX *in vitro* as well as by the proteasome *in vivo* [35,184]. Thus, usage of an FP that is efficiently processed by the protease of choice is a critical consideration prior to an investigation aiming at determination of protein stability. This is not only the case for usage of a tFT, but also for assays that use ratiometric generation of an internal control. In the latter case, an inefficiently digested FP like sfGFP should be avoided as direct fusion partner of the POI. For a tFT assay, placement of sfGFP distal to the degradation initiation site is recommended [35].

For the purpose of protein degradation assays, it would be advantageous to have a more thorough biophysical characterization of the permutated sfGFP variants with respect to maturation time and brightness. At the moment, the available information is incomplete [35,51]. Moreover, incomplete proteolysis of other fluorophores might confer a problem if they are used together with e.g. sfGFP. For mCherry this might not be an issue, as incomplete proteasomal degradation was not detected in the context of tFTs [35]. Yet, no information is available about *in vivo* proteolysis of other, more modern RFPs like Scarlet or Scarlet-I that are increasingly used instead of mCherry due to their higher brightness [84,185–187]. Another issue that needs to be considered before the usage of fluorophores is autofragmentation of FPs [15,188]. This may not be a problem during fluorescent assays, but it can hamper other techniques like immunodetection. For eGFP, the fragments are a

byproduct of autocatalytic chromophore formation. As different FPs show differences in fragment formation, future improvement of FPs may address this issue as well.

Biophysical properties of FPs have to be considered for many applications. These include fluorescence changes induced by pH and oxidation, which depend on the cellular environment of the FP or differences in fluorescence lifetime [189,190]. FPs sensitive to changes in pH and oxidation state have been developed and characterized based on these changes in fluorescence intensity [191–194]. Careful consideration of these properties is required for the interpretation of results originating from large-scale protein degradation assays in system biology. An FP fused to POIs that originate from different cellular environments with differences in pH or redox conditions might show a huge POI-dependent change in fluorescence. Failure to compensate for such influences might lead to an increase of false positive or false negative hits. Usage of organelle specific probes that are optimized for a distinct cellular environment would be one possible solution for such issues. However, properties like pH-dependent shifts in fluorescence lifetime of GFP have been used to monitor events like bacterial phagocytosis [195], which exemplifies the possibilities that careful considerations of biophysical properties of GFP and related proteins are offering.

Moreover, application of FPs in the secretory system is challenged by mechanisms like glycosylation and disulfide bond formation, which both might interfere with FP folding or lead to oligomerization [196]. Oligomerization of eGFP by disulfide bond formation has been observed in endocrine cells, which was resolved by mutation of two cysteines (Cys49, Cys71) [197]. However, cell type specific factors and the exact FP variant might play a role as well, as GFPuv has been reported as a tool to investigate secretion in cultivated insect cells and *Aequorea victoria* GFP has been used to image the secretory pathway in tobacco leaves [198,199]. A toolbox of common FPs and photoswitchable FPs have been developed that are optimized for organelles of the secretory pathways and as fusion partners for membrane proteins [65,200–202]. Yet, variants of the FP Venus or its split variant have been developed whose fluorescence relies on a cycle of glycosylation and deglycosylation [203]. These variants were used to investigate protein degradation via the ERAD pathway. Another method to detect protein-protein interactions, the so called fluorescence resonance energy transfer (FRET), has been used to determine specificity of protein aggregation [204]. The latter process is induced upon failure of proteasomal degradation for certain proteins [205]. During FRET, energy is transferred nonradiatively from a donor FP in its excited state to an excitable FP (the acceptor) and the transfer is highly sensitive to the distance and orientation of the FPs [206]. This aspect is often problematic for successful *in vivo* applications, but the high sensitivity of the method reports accurately about changes in protein-protein interactions.

The researcher investigating protein degradation has a demand for fast-maturing FPs with high brightness, high photostability, no tendency for oligomerization, and smooth proteasomal proteolysis. Yet, the wealth of data produced by tFT assays demonstrates that FPs with diverse maturation times are also interesting for generating reporters with distinct features optimal for illuminating the biological question of interest.

Acknowledgments

The authors thank Alexander Monroe for critical reading of the manuscript. This work was supported by the Deutsche Forschungsgemeinschaft grant TA320-7-1 and the BMBF grant 031B0358A.

Conflict of interest

The authors declare no conflict of interest.

References

1. Mishin AS, Belousov VV, Solntsev KM, et al. (2015) Novel uses of fluorescent proteins. *Curr Opin Chem Biol* 27: 1–9.
2. Shcherbakova DM, Baloban M, Verkhusha VV (2015) Near-infrared fluorescent proteins engineered from bacterial phytochromes. *Curr Opin Chem Biol* 27: 52–63.
3. Rodriguez EA, Campbell RE, Lin JY, et al. (2017) The growing and glowing toolbox of fluorescent and photoactive proteins. *Trends Biochem Sci* 42: 111–129.
4. Hampton RY, Koning A, Wright R, et al. (1996) In vivo examination of membrane protein localization and degradation with green fluorescent protein. *Proc Natl Acad Sci* 93: 828–833.
5. Terskikh A, Fradkov A, Ermakova G, et al. (2000) 'Fluorescent timer': Protein that changes color with time. *Science* 290: 1585–1588.
6. Subach FV, Subach OM, Gundorov IS, et al. (2009) Monomeric fluorescent timers that change color from blue to red report on cellular trafficking. *Nat Chem Biol* 5: 118–126.
7. Khmelinskii A, Keller PJ, Bartosik A, et al. (2012) Tandem fluorescent protein timers for in vivo analysis of protein dynamics. *Nat Biotechnol* 30: 708–714.
8. Zhang L, Gurskaya NG, Merzlyak EM, et al. (2007) Method for real-time monitoring of protein degradation at the single cell level. *Biotechniques* 42: 446–450.
9. Taxis C, Hitt R, Park SH, et al. (2003) Use of modular substrates demonstrates mechanistic diversity and reveals differences in chaperone requirement of ERAD. *J Biol Chem* 278: 35903–35913.
10. Balleza E, Kim JM, Cluzel P (2018) Systematic characterization of maturation time of fluorescent proteins in living cells. *Nat Methods* 15: 47–51.
11. Maeder CI, Hink MA, Kinkhabwala A, et al. (2007) Spatial regulation of Fus3 MAP kinase activity through a reaction-diffusion mechanism in yeast pheromone signalling. *Nat Cell Biol* 9: 1319–1326.
12. Subach OM, Cranfill PJ, Davidson MW, et al. (2011) An enhanced monomeric blue fluorescent protein with the high chemical stability of the chromophore. *PLoS One* 6: e28674.
13. Langan RA, Boyken SE, Ng AH, et al. (2019) De novo design of bioactive protein switches. *Nature* 572: 205–210.
14. Subach OM, Gundorov IS, Yoshimura M, et al. (2008) Conversion of red fluorescent protein into a bright blue probe. *Chem Biol* 15: 1116–1124.
15. Wei J, Gibbs JS, Hickman HD, et al. (2015) Ubiquitous autofragmentation of fluorescent proteins creates abundant defective ribosomal products (DRiPs) for immunosurveillance. *J Biol Chem* 290: 16431–16439.
16. Goedhart J, Von Stetten D, Noirclerc-Savoye M, et al. (2012) Structure-guided evolution of cyan fluorescent proteins towards a quantum yield of 93%. *Nat Commun* 3: 751.
17. Ng AH, Nguyen TH, Gómez-Schiavon M, et al. (2019) Modular and tunable biological feedback control using a de novo protein switch. *Nature* 572: 265–269.

18. Heim R, Tsien RY (1996) Engineering green fluorescent protein for improved brightness, longer wavelengths and fluorescence resonance energy transfer. *Curr Biol* 6: 178–182.
19. Rizzo MA, Springer GH, Granada B, et al. (2004) An improved cyan fluorescent protein variant useful for FRET. *Nat Biotechnol* 22: 445–449.
20. Cubitt AB, Woollenweber LA, Heim R (1998) Understanding structure-function relationships in the Aequorea victoria green fluorescent protein. *Methods Cell Biol* 58: 19–30.
21. Patterson G, Day RN, Piston D (2001) Fluorescent protein spectra. *J Cell Sci* 114: 837–838.
22. Cookson NA, Mather WH, Danino T, et al. (2011) Queueing up for enzymatic processing: correlated signaling through coupled degradation. *Mol Syst Biol* 7: 561.
23. Jungbluth M, Renicke C, Taxis C (2010) Targeted protein depletion in Saccharomyces cerevisiae by activation of a bidirectional degron. *BMC Syst Biol* 4: 176.
24. Taxis C, Stier G, Spadaccini R, et al. (2009) Efficient protein depletion by genetically controlled deprotection of a dormant N-degron. *Mol Syst Biol* 5: 267.
25. Hasenjäger S, Trauth J, Hepp S, et al. (2019) Optogenetic downregulation of protein levels with an ultrasensitive switch. *ACS Synth Biol* 8: 1026–1036.
26. Cormack BP, Valdivia RH, Falkow S (1996) FACS-optimized mutants of the green fluorescent protein (GFP). *Gene* 173: 33–38.
27. Pepperkok R, Squire A, Geley S, et al. (1999) Simultaneous detection of multiple green fluorescent proteins in live cells by fluorescence lifetime imaging microscopy. *Curr Biol* 9: 269–272.
28. Seefeldt B, Kasper R, Seidel T, et al. (2008) Fluorescent proteins for single-molecule fluorescence applications. *J Biophotonics* 1: 74–82.
29. Sarkisyan KS, Goryashchenko AS, Lidsky PV, et al. (2015) Green fluorescent protein with anionic tryptophan-based chromophore and long fluorescence lifetime. *Biophys J* 109: 380–389.
30. Halter M, Tona A, Bhadriraju K, et al. (2007) Automated live cell imaging of green fluorescent protein degradation in individual fibroblasts. *Cytom Part A: J Int Soc Anal Cytol* 71: 827–834.
31. Yen HCS, Xu Q, Chou DM, et al. (2008) Global protein stability profiling in mammalian cells. *Science* 322: 918–923.
32. Yen HCS, Elledge SJ (2008) Identification of SCF ubiquitin ligase substrates by global protein stability profiling. *Science* 322: 923–929.
33. Reichard EL, Chirico GG, Dewey WJ, et al. (2016) Substrate ubiquitination controls the unfolding ability of the proteasome. *J Biol Chem* 291: 18547–18561.
34. Lin HC, Yeh CW, Chen YF, et al. (2018) C-terminal end-directed protein elimination by CRL2 ubiquitin ligases. *Mol Cell* 70: 602–613.
35. Khmelinskii A, Meurer M, Ho CT, et al. (2016) Incomplete proteasomal degradation of green fluorescent proteins in the context of tandem fluorescent protein timers. *Mol Biol Cell* 27: 360–370.
36. Krentz NAJ, van Hoof D, Li Z, et al. (2017) Phosphorylation of NEUROG3 links endocrine differentiation to the cell cycle in pancreatic progenitors. *Dev Cell* 41: 129–142.
37. Link CD, Fonte V, Hiester B, et al. (2006) Conversion of green fluorescent protein into a toxic, aggregation-prone protein by C-terminal addition of a short peptide. *J Biol Chem* 281: 1808–1816.
38. Papagiannakis A, de Jonge JJ, Zhang Z, et al. (2017) Quantitative characterization of the auxin-inducible degron: a guide for dynamic protein depletion in single yeast cells. *Sci Rep* 7: 1–13.

39. Usherenko S, Stibbe H, Muscò M, et al. (2014) Photo-sensitive degron variants for tuning protein stability by light. *BMC Syst Biol* 8: 128.
40. Qian SB, Ott DE, Schubert U, et al. (2002) Fusion proteins with COOH-terminal ubiquitin are stable and maintain dual functionality in vivo. *J Biol Chem* 277: 38818–38826.
41. Li X, Zhao X, Fang Y, et al. (1998) Generation of destabilized green fluorescent protein as a transcription reporter. *J Biol Chem* 273: 34970–34975.
42. Iconomou M, Saunders DN (2016) Systematic approaches to identify E3 ligase substrates. *Biochem J* 473: 4083–4101.
43. Shaner NC, Lin MZ, McKeown MR, et al. (2008) Improving the photostability of bright monomeric orange and red fluorescent proteins. *Nat Methods* 5: 545–551.
44. Zacharias DA, Violin JD, Newton AC, et al. (2002) Partitioning of lipid-modified monomeric GFPs into membrane microdomains of live cells. *Science* 296: 913–916.
45. Shimomura O, Johnson F H, Saiga Y (1962) Extraction, purification and properties of aequorin, a bioluminescent protein from the luminous hydromedusan, Aequorea. *J Cell Comp Physiol* 59: 223–239.
46. Niwa H, Inouye S, Hirano T, et al. (1996) Chemical nature of the light emitter of the Aequorea green fluorescent protein. *Proc Natl Acad Sci* 93: 13617–13622.
47. Prasher DC, Eckenrode VK, Ward WW, et al. (1992) Primary structure of the Aequorea victoria green-fluorescent protein. *Gene* 111: 229–233.
48. Patterson GH, Knobel SM, Sharif WD, et al. (1997) Use of the green fluorescent protein and its mutants in quantitative fluorescence microscopy. *Biophys J* 73: 2782–2790.
49. Iizuka R, Yamagishi-Shirasaki M, Funatsu T (2011) Kinetic study of de novo chromophore maturation of fluorescent proteins. *Anal Biochem* 414: 173–178.
50. Yoo TH, Link AJ, Tirrell DA (2007) Evolution of a fluorinated green fluorescent protein. *Proc Natl Acad Sci* 104: 13887–13890.
51. Pédelacq JD, Cabantous S, Tran T, et al. (2006) Engineering and characterization of a superfolder green fluorescent protein. *Nat Biotechnol* 24: 79–88.
52. Durrieu L, Kirrmaier D, Schneidt T, et al. (2018) Bicoid gradient formation mechanism and dynamics revealed by protein lifetime analysis. *Mol Syst Biol* 14: e8355.
53. Kowalski L, Bragoszewski P, Khmelinskii A, et al. (2018) Determinants of the cytosolic turnover of mitochondrial intermembrane space proteins. *BMC Biol* 16: 66.
54. Dederer V, Khmelinskii A, Huhn AG, et al. (2019) Cooperation of mitochondrial and ER factors in quality control of tail-anchored proteins. *Elife* 8: e45506.
55. Alber AB, Paquet ER, Biserni M, et al. (2018) Single live cell monitoring of protein turnover reveals intercellular variability and cell-cycle dependence of degradation rates. *Mol Cell* 71: 1079–1091.
56. Zhang H, Linster E, Gannon L, et al. (2019) Tandem fluorescent protein timers for noninvasive relative protein lifetime measurement in plants. *Plant Physiol* 180: 718–731.
57. Fernandez-Rodriguez J, Voigt CA (2016) Post-translational control of genetic circuits using Potyvirus proteases. *Nucleic Acids Res* 44: 6493–6502.
58. Yu H, Singh Gautam AKS, Wilmington SR, et al. (2016) Conserved sequence preferences contribute to substrate recognition by the proteasome. *J Biol Chem* 291: 14526–14539.
59. Donà E, Barry JD, Valentin G, et al. (2013) Directional tissue migration through a self-generated chemokine gradient. *Nature* 503: 285–289.

60. Khmelinskii A, Blaszczak E, Pantazopoulou M, et al. (2014) Protein quality control at the inner nuclear membrane. *Nature* 516: 410–413.
61. Kats I, Khmelinskii A, Kschonsak M, et al. (2018) Mapping degradation signals and pathways in a eukaryotic N-terminome. *Mol Cell* 70: 488–501.
62. Castells-Ballester J, Zatorska E, Meurer M, et al. (2018) Monitoring protein dynamics in protein o-mannosyltransferase mutants in vivo by tandem fluorescent protein timers. *Molecules* 23: 2622.
63. Heim R, Cubitt AB, Tsien RY (1995) Improved green fluorescence. *Nature* 373: 663–664.
64. Benanti JA, Cheung SK, Brady MC, et al. (2007) A proteomic screen reveals SCFGrr1 targets that regulate the glycolytic-gluconeogenic switch. *Nat Cell Biol* 9: 1184–1191.
65. Costantini LM, Baloban M, Markwardt ML, et al. (2015) A palette of fluorescent proteins optimized for diverse cellular environments. *Nat Commun* 6: 7670.
66. Kremers GJ, Goedhart J, van den Heuvel DJ, et al. (2007) Improved green and blue fluorescent proteins for expression in bacteria and mammalian cells. *Biochemistry* 46: 3775–3783.
67. Sekar K, Gentile AM, Bostick JW, et al. (2016) N-terminal-based targeted, inducible protein degradation in Escherichia coli. *PLoS One* 11: e0149746.
68. Shaner NC, Lambert GG, Chammas A, et al. (2013) A bright monomeric green fluorescent protein derived from Branchiostoma lanceolatum. *Nat Methods* 10: 407–409.
69. Molina RS, Tran TM, Campbell RE, et al. (2017) Blue-shifted green fluorescent protein homologues are brighter than enhanced green fluorescent protein under two-photon excitation. *J Phys Chem Lett* 8: 2548–2554.
70. Griesbeck O, Baird GS, Campbell RE, et al. (2001) Reducing the environmental sensitivity of yellow fluorescent protein mechanism and applications. *J Biol Chem* 276: 29188–29194.
71. Wiens MD, Hoffmann F, Chen Y, et al. (2018) Enhancing fluorescent protein photostability through robot-assisted photobleaching. *Integr Biol* 10: 419–428.
72. Cranfill PJ, Sell BR, Baird MA, et al. (2016) Quantitative assessment of fluorescent proteins. *Nat Methods* 13: 557–562.
73. Miyawaki A, Griesbeck O, Heim R, et al. (1999) Dynamic and quantitative Ca^{2+} measurements using improved cameleons. *Proc Natl Acad Sci* 96: 2135–2140.
74. Ormö M, Cubitt AB, Kallio K, et al. (1996) Crystal structure of the aequorea victoria green fluorescent protein. *Science* 273: 1392–1395.
75. Rekas A, Alattia JR, Nagai T, et al. (2002) Crystal structure of venus, a yellow fluorescent protein with improved maturation and reduced environmental sensitivity. *J Biol Chem* 277: 50573–50578.
76. Zhao W, Pferdehirt L, Segatori L (2018) Quantitatively predictable control of cellular protein levels through proteasomal degradation. *ACS Synth Biol* 7: 540–552.
77. Eden E, Geva-Zatorsky N, Issaeva I, et al. (2011) Proteome half-life dynamics in living human cells. *Science* 331: 764–768.
78. Nagai T, Ibata K, Park ES, et al. (2002) A variant of yellow fluorescent protein with fast and efficient maturation for cell-biological applications. *Nat Biotechnol* 20: 87–90.
79. Chassin H, Müller M, Tigges M, et al. (2019) A modular degron library for synthetic circuits in mammalian cells. *Nat Commun* 10: 2013.
80. Shaner NC, Campbell RE, Steinbach P a, et al. (2004) Improved monomeric red, orange and yellow fluorescent proteins derived from Discosoma sp. red fluorescent protein. *Nat Biotechnol* 22: 1567–1572.

81. Merzlyak EM, Goedhart J, Shcherbo D, et al. (2007) Bright monomeric red fluorescent protein with an extended fluorescence lifetime. *Nat Methods* 4: 555–557.
82. Renicke C, Schuster D, Usherenko S, et al. (2013) A LOV2 domain-based optogenetic tool to control protein degradation and cellular function. *Chem Biol* 20: 619–626.
83. Strack RL, Strongin DE, Bhattacharyya D, et al. (2008) A noncytotoxic DsRed variant for whole-cell labeling. *Nat Methods* 5: 955–957.
84. Bindels DS, Haarbosch L, van Weeren L, et al. (2017) mScarlet: a bright monomeric red fluorescent protein for cellular imaging. *Nat Methods* 14: 53–56.
85. Campbell RE, Tour O, Palmer AE, et al. (2002) A monomeric red fluorescent protein. *Proc Natl Acad Sci* 99: 7877–7882.
86. Shcherbo D, Murphy CS, Ermakova GV, et al. (2009) Far-red fluorescent tags for protein imaging in living tissues. *Biochem J* 418: 567–574.
87. Shcherbo D, Merzlyak EM, Chepurnykh TV, et al. (2007) Bright far-red fluorescent protein for whole-body imaging. *Nat Methods* 4: 741–746.
88. Filonov GS, Piatkevich KD, Ting L-M, et al. (2011) Bright and stable near-infrared fluorescent protein for in vivo imaging. *Nat Biotechnol* 29: 757–761.
89. Nemet I, Ropelewski P, Imanishi Y (2015) Applications of phototransformable fluorescent proteins for tracking the dynamics of cellular components. *Photochem Photobiol Sci* 14: 1787–1806.
90. Vilchez D, Saez I, Dillin A (2014) The role of protein clearance mechanisms in organismal ageing and age-related diseases. *Nat Commun* 5: 5659.
91. Hershko A, Ciechanover A (1998) The ubiquitin system. *Annu Rev Biochem* 67: 425–479.
92. Pickart CM (2004) Back to the future with ubiquitin. *Cell* 116: 181–190.
93. Ardley HC, Robinson PA (2005) E3 ubiquitin ligases. *Essays Biochem* 41: 15–30.
94. Metzger MB, Pruneda JN, Klevit RE, et al. (2014) RING-type E3 ligases: Master manipulators of E2 ubiquitin-conjugating enzymes and ubiquitination. *Biochim Biophys Acta-Mol Cell Res* 1843: 47–60.
95. Thrower JS, Hoffman L, Rechsteiner M, et al. (2000) Recognition of the polyubiquitin proteolytic signal. *EMBO J* 19: 94–102.
96. Yau R, Rape M (2016) The increasing complexity of the ubiquitin code. *Nat Cell Biol* 18: 579–586.
97. Kwon YT, Ciechanover A (2017) The ubiquitin code in the ubiquitin-proteasome system and autophagy. *Trends Biochem Sci* 42: 873–886.
98. Yu H, Matouschek A (2017) Recognition of client proteins by the proteasome. *Annu Rev Biophys* 46: 149–173.
99. Varshavsky A (1991) Naming a targeting signal. *Cell* 64: 13–15.
100. Ravid T, Hochstrasser M (2008) Diversity of degradation signals in the ubiquitin-proteasome system. *Nat Rev Mol Cell Biol* 9: 679–689.
101. Tomita T, Matouschek A (2019) Substrate selection by the proteasome through initiation regions. *Protein Sci* 28: 1222–1232.
102. Jariel-Encontre I, Bossis G, Piechaczyk M (2008) Ubiquitin-independent degradation of proteins by the proteasome. *Biochim Biophys Acta - Rev Cancer* 1786: 153–177.
103. Erales J, Coffino P (2014) Ubiquitin-independent proteasomal degradation. *Biochim Biophys Acta-Mol Cell Res* 1843: 216–221.

104. Dohmen RJ, Willers I, Marques AJ (2007) Biting the hand that feeds: Rpn4-dependent feedback regulation of proteasome function. *Biochim Biophys Acta-Mol Cell Res* 1773: 1599–1604.
105. Ha SW, Ju D, Xie Y (2012) The N-terminal domain of Rpn4 serves as a portable ubiquitin-independent degron and is recognized by specific 19S RP subunits. *Biochem Biophys Res Commun* 419: 226–231.
106. Lutz AP, Schladebeck S, Renicke C, et al. (2018) Proteasome activity is influenced by the HECT_2 protein Ipa1 in budding yeast. *Genetics* 209: 157–171.
107. Scheffer J, Hasenjäger S, Taxis C (2019) Degradation of integral membrane proteins modified with the photosensitive degron module requires the cytosolic endoplasmic reticulum–associated degradation pathway. *Mol Biol Cell* 30: 2558–2570.
108. Hitchcock AL, Krebber H, Frietze S, et al. (2001) The conserved npl4 protein complex mediates proteasome-dependent membrane-bound transcription factor activation. *Mol Biol Cell* 12: 3226–3241.
109. Hoppe T, Matuschewski K, Rape M, et al. (2001) Activation of a membrane-bound transcription factor by regulated ubiquitin/proteasome-dependent processing. *Cell* 14: 148–151.
110. Leestemaker Y, Ovaa H (2017) Tools to investigate the ubiquitin proteasome system. *Drug Discov Today Technol* 26: 25–31.
111. Conole D, Mondal M, Majmudar JD, et al. (2019) Recent developments in cell permeable deubiquitinating enzyme activity-based probes. *Front Chem* 7: 876.
112. Hewings DS, Flygare JA, Bogyo M, et al. (2017) Activity-based probes for the ubiquitin conjugation-deconjugation machinery: new chemistries, new tools, and new insights. *FEBS J* 284: 1555–1576.
113. Ella H, Reiss Y, Ravid T (2019) The hunt for degrons of the 26S proteasome. *Biomolecules* 9: 230.
114. Chalfie M, Tu Y, Euskirchen G, et al. (1994) Green fluorescent protein as a marker for gene expression. *Science* 263: 802–805.
115. Wang S, Hazelrigg T (1994) Implications for bcd mRNA localization from spatial distribution of exu protein in Drosophila oogenesis. *Nature* 369: 400–403.
116. Cronin SR, Hampton RY (1999) Measuring protein degradation with green fluorescent protein. *Methods Enzymol* 302: 58–73.
117. Cronin SR, Khoury A, Ferry DK, et al. (2000) Regulation of HMG-CoA reductase degradation requires the P-type ATPase Cod1p/Spf1p. *J Cell Biol* 148: 915–924.
118. Jiang X, Coffino P, Li X (2004) Development of a method for screening short-lived proteins using green fluorescent protein. *Genome Biol* 5: R81.
119. Hampton RY, Rine J (1994) Regulated degradation of HMG-CoA reductase, an integral membrane protein of the endoplasmic reticulum, in yeast. *J Cell Biol* 125: 299–312.
120. Gierisch ME, Giovannucci TA, Dantuma NP (2020) Reporter-based screens for the ubiquitin/proteasome system. *Front Chem* 8: 64.
121. Dantuma NP, Lindsten K, Glas R, et al. (2000) Short-lived green fluorescent proteins for quantifying ubiquitin/proteasome-dependent proteolysis in living cells. *Nat Biotechnol* 18: 538–543.
122. van Wijk SJ, Fulda S, Dikic I, et al. (2019) Visualizing ubiquitination in mammalian cells. *EMBO Rep* 20: e46520.
123. Rajan S, Djambazian H, Dang HCP, et al. (2011) The living microarray: A high-throughput platform for measuring transcription dynamics in single cells. *BMC Genomics* 12: 115.

124. Chou TF, Deshaies RJ (2011) Quantitative cell-based protein degradation assays to identify and classify drugs that target the ubiquitin-proteasome system. *J Biol Chem* 286: 16546–16554.
125. He L, Binari R, Huang J, et al. (2019) In vivo study of gene expression with an enhanced dual-color fluorescent transcriptional timer. *Elife* 8: e46181.
126. Mei L, Fan Y, Lv X, et al. (2018) Long-term in vivo recording of circadian rhythms in brains of freely moving mice. *Proc Natl Acad Sci* 115: 4276–4281.
127. Ando H, Hirose M, Kurosawa G, et al. (2017) Time-lapse imaging of microRNA activity reveals the kinetics of microRNA activation in single living cells. *Sci Rep* 7: 1–16.
128. Sharifnia P, Kim KW, Wu Z, et al. (2017) Distinct cis elements in the 3′ UTR of the C. elegans cebp-1 mRNA mediate its regulation in neuronal development. *Dev Biol* 429: 240–248.
129. Toneff MJ, Sreekumar A, Tinnirello A, et al. (2016) The Z-cad dual fluorescent sensor detects dynamic changes between the epithelial and mesenchymal cellular states. *BMC Biol* 14: 47.
130. Stacer AC, Wang H, Fenner J, et al. (2015) Imaging reporters for proteasome activity identify tumor- and metastasis-initiating cells. *Mol Imaging* 14: 414–428.
131. Langenbach KJ, Elliott JT, Tona A, et al. (2006) Thin films of type 1 collagen for cell by cell analysis of morphology and tenascin-C promoter activity. *BMC Biotechnol* 6: 14.
132. Raser JM, O'Shea EK (2005) Noise in gene expression: Origins, consequences, and control. *Science* 309: 2010–2013.
133. Deng W, Bates JA, Wei H, et al. (2020) Tunable light and drug induced depletion of target proteins. *Nat Commun* 11: 304.
134. Gilon T, Chomsky O, Kulka RG (2000) Degradation signals recognized by the Ubc6p-Ubc7p ubiquitin-conjugating enzyme pair. *Mol Cell Biol* 20: 7214–7219.
135. Bence NF, Sampat RM, Kopito RR (2001) Impairment of the ubiquitin-proteasome system by protein aggregation. *Science* 292: 1552–1555.
136. Schipper-Krom S, Sanz AS, van Bodegraven EJ, et al. (2019) Visualizing proteasome activity and intracellular localization using fluorescent proteins and activity-based probes. *Front Mol Biosci* 6: 56.
137. Dyson MR (2016) Fundamentals of expression in mammalian cells, *Advances in Experimental Medicine and Biology*, Switzerland: Springer, 217–224.
138. Voss U, Larrieu A, Wells DM (2013) From jellyfish to biosensors: The use of fluorescent proteins in plants. *Int J Dev Biol* 57: 525–533.
139. Colman-Lerner A, Gordon A, Serra E, et al. (2005) Regulated cell-to-cell variation in a cell-fate decision system. *Nature* 437: 699–706.
140. Gordon A, Colman-lerner A, Chin TE, et al. (2007) Single-cell quantification of molecules and rates using open-source microscope-based cytometry. *Nat Methods* 4: 175–181.
141. Grossmann G, Krebs M, Maizel A, et al. (2018) Green light for quantitative live-cell imaging in plants. *J Cell Sci* 131: jcs209270.
142. Croce AC, Bottiroli G (2017) Autofluorescence spectroscopy for monitoring metabolism in animal cells and tissues, *Histochemistry of Single Molecules*, New York: Humana Press, 15–43.
143. Feuchtinger A, Walch A, Dobosz M (2016) Deep tissue imaging: a review from a preclinical cancer research perspective. *Histochem Cell Biol* 146: 781–806.
144. Zhao W, Bonem M, McWhite C, et al. (2014) Sensitive detection of proteasomal activation using the Deg-On mammalian synthetic gene circuit. *Nat Commun* 5: 3612.
145. Adam V, Nienhaus K, Bourgeois D, et al. (2009) Structural basis of enhanced photoconversion yield in green fluorescent protein-like protein Dendra2. *Biochemistry* 48: 4905–4915.

146. Adam V, Moeyaert B, David CC, et al. (2011) Rational design of photoconvertible and biphotochromic fluorescent proteins for advanced microscopy applications. *Chem Biol* 18: 1241–1251.
147. Gurskaya NG, Verkhusha VV, Shcheglov AS, et al. (2006) Engineering of a monomeric green-to-red photoactivatable fluorescent protein induced by blue light. *Nat Biotechnol* 24: 461–465.
148. Hoi H, Shaner NC, Davidson MW, et al. (2010) A monomeric photoconvertible fluorescent protein for imaging of dynamic protein localization. *J Mol Biol* 401: 776–791.
149. Hamer G, Matilainen O, Holmberg CI (2010) A photoconvertible reporter of the ubiquitin-proteasome system in vivo. *Nat Methods* 7: 473–478.
150. Patterson GH, Lippincott-Schwartz J (2002) A photoactivatable GFP for selective photolabeling of proteins and cells. *Science* 297: 1873–1877.
151. Heidary DK, Fox A, Richards CI, et al. (2017) A high-throughput screening assay using a photoconvertable protein for identifying inhibitors of transcription, translation, or proteasomal degradation. *SLAS Discov* 22: 399–407.
152. Kiuchi T, Nagai T, Ohashi K, et al. (2011) Measurements of spatiotemporal changes in G-actin concentration reveal its effect on stimulus-induced actin assembly and lamellipodium extension. *J Cell Biol* 193: 365–380.
153. Drocco JA, Grimm O, Tank DW, et al. (2011) Measurement and perturbation of morphogen lifetime: Effects on gradient shape. *Biophys J* 101: 1807–1815.
154. Rogers KW, Bläße A, Schier AF, et al. (2015) Measuring protein stability in living zebrafish embryos using fluorescence decay after photoconversion (FDAP). *JoVE* 95: e52266.
155. Plachta N, Bollenbach T, Pease S, et al. (2011) Oct4 kinetics predict cell lineage patterning in the early mammalian embryo. *Nat Cell Biol* 13: 117–123.
156. Goldberg AL, Dice JF (1974) Intracellular protein degradation in mammalian and bacterial cells. *Annu Rev Biochem* 43: 835–869.
157. Schimke RT, Doyle D (1970) Control of enzyme levels in animal tissues. *Annu Rev Biochem* 39: 929–976.
158. McShane E, Sin C, Zauber H, et al. (2016) Kinetic analysis of protein stability reveals age-dependent degradation. *Cell* 167: 803–815.e21.
159. Verzijlbergen KF, Menendez-Benito V, van Welsem T, et al. (2010) Recombination-induced tag exchange to track old and new proteins. *Proc Natl Acad Sci* 107: 64–68.
160. Buchwalter A, Schulte R, Tsai H, et al. (2019) Selective clearance of the inner nuclear membrane protein emerin by vesicular transport during ER stress. *Elife* 8: e49796.
161. Toyama BH, Drigo RA, Lev-Ram V, et al. (2019) Visualization of long-lived proteins reveals age mosaicism within nuclei of postmitotic cells. *J Cell Biol* 218: 433–444.
162. van Deventer S, Menendez-Benito V, van Leeuwen F, et al. (2015) N-terminal acetylation and replicative age affect proteasome localization and cell fitness during aging. *J Cell Sci* 128: 109–117.
163. Hughes AL, Hughes CE, Henderson KA, et al. (2016) Selective sorting and destruction of mitochondrial membrane proteins in aged yeast. *Elife* 5: e13943.
164. Thayer NH, Leverich CK, Fitzgibbon MP, et al. (2014) Identification of long-lived proteins retained in cells undergoing repeated asymmetric divisions. *Proc Natl Acad Sci* 111: 14019–14026.

165. Koren I, Timms RT, Kula T, et al. (2018) The eukaryotic proteome is shaped by E3 ubiquitin ligases targeting C-terminal Degrons. *Cell* 173: 1622–1635.e14.
166. Wilmington SR, Matouschek A (2016) An inducible system for rapid degradation of specific cellular proteins using proteasome adaptors. *PLoS One* 11: e0152679.
167. Mizuguchi H, Xu Z, Ishii-Watabe A, et al. (2000) IRES-dependent second gene expression is significantly lower than cap-dependent first gene expression in a bicistronic vector. *Mol Ther* 1: 376–382.
168. Wong ET, Ngoi SM, Lee CGL (2002) Improved co-expression of multiple genes in vectors containing internal ribosome entry sites (IRESes) from human genes. *Gene Ther* 9: 337–344.
169. Licursi M, Christian SL, Pongnopparat T, et al. (2011) In vitro and in vivo comparison of viral and cellular internal ribosome entry sites for bicistronic vector expression. *Gene Ther* 18: 631–636.
170. Koh EYC, Ho SCL, Mariati, et al. (2013) An internal ribosome entry site (IRES) mutant library for tuning expression level of multiple genes in mammalian cells. *PLoS One* 8: e82100.
171. Chappell SA, Edelman GM, Mauro VP (2000) A 9-nt segment of a cellular mRNA can function as an internal ribosome entry site (IRES) and when present in linked multiple copies greatly enhances IRES activity. *Proc Natl Acad Sci* 97: 1536–1541.
172. Hennecke M (2001) Composition and arrangement of genes define the strength of IRES-driven translation in bicistronic mRNAs. *Nucleic Acids Res* 29: 3327–3334.
173. Al-Allaf FA, Abduljaleel Z, Athar M, et al. (2019) Modifying inter-cistronic sequence significantly enhances IRES dependent second gene expression in bicistronic vector: Construction of optimised cassette for gene therapy of familial hypercholesterolemia. *Non-coding RNA Res* 4: 1–14.
174. Kim JH, Lee SR, Li LH, et al. (2011) High cleavage efficiency of a 2A peptide derived from porcine teschovirus-1 in human cell lines, zebrafish and mice. *PLoS One* 6: 1–8.
175. De Felipe P, Luke GA, Brown JD, et al. (2010) Inhibition of 2A-mediated 'cleavage' of certain artificial polyproteins bearing N-terminal signal sequences. *Biotechnol J* 5: 213–223.
176. Lo CA, Kays I, Emran F, et al. (2015) Quantification of protein levels in single living cells. *Cell Rep* 13: 2634–2644.
177. de Felipe P (2004) Skipping the co-expression problem: The new 2A 'CHYSEL' technology. *Genet Vaccines Ther* 2: 13.
178. Luke GA, Ryan MD (2018) Using the 2A protein coexpression system: Multicistronic 2A vectors expressing gene(s) of interest and reporter proteins, *Reporter Gene Assays*, New York: Humana Press, 31–48.
179. Kreidenweiss A, Hopkins A V., Mordmüller B (2013) 2A and the auxin-based degron system facilitate control of protein levels in Plasmodium falciparum. *PLoS One* 8: 2–7.
180. Hepp S, Trauth J, Hasenjäger S, et al. (2020) An optogenetic tool for induced protein stabilization based on the Phaeodactylum tricornutum aureochrome 1a LOV domain. *J Mol Biol*.
181. Yu H, Kago G, Yellman CM, et al. (2016) Ubiquitin-like domains can target to the proteasome but proteolysis requires a disordered region. *EMBO J* 35: 1522–1536.
182. Fernandes AC, Uytterhoeven V, Kuenen S, et al. (2014) Reduced synaptic vesicle protein degradation at lysosomes curbs TBC1D24/sky-induced neurodegeneration. *J Cell Biol* 207: 453–462.
183. Saeki Y, Kudo T, Sone T, et al. (2009) Lysine 63-linked polyubiquitin chain may serve as a targeting signal for the 26S proteasome. *EMBO J* 28: 359–371.

184. Nager AR, Baker TA, Sauer RT (2011) Stepwise unfolding of a β barrel protein by the AAA+ ClpXP protease. *J Mol Biol* 413: 4–16.
185. Yamaguchi N, Colak-Champollion T, Knaut H (2019) zGrad is a nanobody-based degron system that inactivates proteins in zebrafish. *Elife* 8: e43125.
186. Botman D, de Groot DH, Schmidt P, et al. (2019) In vivo characterisation of fluorescent proteins in budding yeast. *Sci Rep* 9: 2234.
187. El Mouridi S, Lecroisey C, Tardy P, et al. (2017) Reliable CRISPR/Cas9 genome engineering in Caenorhabditis elegans using a single efficient sgRNA and an easily recognizable phenotype. *G3: Genes, Genomes, Genetics* 7: 1429–1437.
188. Barondeau DP, Kassmann CJ, Tainer J a, et al. (2006) Understanding GFP posttranslational chemistry: structures of designed variants that achieve backbone fragmentation, hydrolysis, and decarboxylation. *J Am Chem Soc* 128: 4685–4693.
189. Chudakov DM, Matz MV., Lukyanov S, et al. (2010) Fluorescent proteins and their applications in imaging living cells and tissues. *Physiol Rev* 90: 1103–1163.
190. Borst JW, Visser AJWG (2010) Fluorescence lifetime imaging microscopy in life sciences. *Meas Sci Technol* 21: 102002.
191. Burgstaller S, Bischof H, Gensch T, et al. (2019) PH-Lemon, a fluorescent protein-based pH reporter for acidic compartments. *ACS Sensors* 4: 883–891.
192. Fan Y, Ai HW (2016) Development of redox-sensitive red fluorescent proteins for imaging redox dynamics in cellular compartments. *Anal Bioanal Chem* 408: 2901–2911.
193. Sugiura K, Tanaka H, Kurisu G, et al. (2019) Multicolor redox sensor proteins can visualize redox changes in various compartments of the living cell. *Biochim Biophys Acta-Gen Subj* 1863: 1098–1107.
194. Germond A, Fujita H, Ichimura T, et al. (2016) Design and development of genetically encoded fluorescent sensors to monitor intracellular chemical and physical parameters. *Biophys Rev* 8: 121–138.
195. Li W, Houston KD, Houston JP (2017) Shifts in the fluorescence lifetime of EGFP during bacterial phagocytosis measured by phase-sensitive flow cytometry. *Sci Rep* 7: 1–11.
196. Costantini LM, Snapp EL (2013) Fluorescent proteins in cellular organelles: Serious pitfalls and some solutions. *DNA Cell Biol* 32: 622–627.
197. Jain RK, Joyce PBM, Molinete M, et al. (2001) Oligomerization of green fluorescent protein in the secretory pathway of endocrine cells. *Biochem J* 360: 645–649.
198. Ashikawa Y, Ihara M, Matsuura N, et al. (2011) GFP-based evaluation system of recombinant expression through the secretory pathway in insect cells and its application to the extracellular domains of class C GPCRs. *Protein Sci* 20: 1720–1734.
199. Boevink P, Martin B, Oparka K, et al. (1999) Transport of virally expressed green fluorescent protein through the secretory pathway in tobacco leaves is inhibited by cold shock and brefeldin A. *Planta* 208: 392–400.
200. Kaberniuk AA, Morano NC, Verkhusha VV, et al. (2017) moxDendra2: an inert photoswitchable protein for oxidizing environments. *Chem Commun* 53: 2106–2109.
201. Costantini LM, Subach OM, Jaureguiberry-bravo M, et al. (2013) Cysteineless non-glycosylated monomeric blue fluorescent protein, secBFP2, for studies in the eukaryotic secretory pathway. *Biochem Biophys Res Commun* 430: 1114–1119.

202. Kaberniuk AA, Mohr MA, Verkhusha VV, et al. (2018) moxMaple3: a photoswitchable fluorescent protein for PALM and protein highlighting in oxidizing cellular environments. *Sci Rep* 8: 1–10.
203. Grotzke JE, Lu Q, Cresswell P (2013) Deglycosylation-dependent fluorescent proteins provide unique tools for the study of ER-associated degradation. *Proc Natl Acad Sci* 110: 3393–3398.
204. Rajan RS, Illing ME, Bence NF, et al. (2001) Specificity in intracellular protein aggregation and inclusion body formation. *Proc Natl Acad Sci* 98: 13060–13065.
205. Trojanowski JQ, Lee VM-Y (2000) "Fatal attractions" of proteins: A comprehensive hypothetical mechanism underlying Alzheimer's disease and other neurodegenerative disorders. *Ann N Y Acad Sci* 924: 62–67.
206. Piston DW, Kremers GJ (2007) Fluorescent protein FRET: the good, the bad and the ugly. *Trends Biochem Sci* 32: 407–414.

AIMS Press